IL NUOVO CIMENTO **39 C** (2016) 303
DOI 10.1393/ncc/i2016-16303-1

COLLOQUIA: SWGM 2015

Investigating protein structure and dynamics through wide-angle X-ray solution scattering

A. CUPANE and M. LEVANTINO(*)

Department of Physics and Chemistry, University of Palermo
Viale delle Scienze - Edificio 18, Palermo 90128, Italy

received 19 July 2016

Summary. — Wide-angle X-ray scattering (WAXS) is a powerful tool that can be used to gain information on the structure and dynamics of proteins and other biomolecules in solution. Improved methods for the calculation of WAXS patterns from available or putative protein models allow to better exploit the structural information contained in the experimental data. These methods, together with recent applications of static and time-resolved WAXS, are briefly reviewed.

1. – Introduction

Proteins are large macromolecules typically made of several thousands atoms that, in order to perform their specific biological function, have to undergo both large-scale conformational changes and more localized structural fluctuations. Investigating the dynamics of these protein motions is crucial to understand protein function [1-3]. In view of the extremely wide range of different time-scales and spatial extent of such motions, experimental techniques that combine high time-resolution with structural sensitivity are required. X-ray scattering from a solution of macromolecules produces a two-dimensional pattern characterized by diffuse rings of scattered intensity (fig. 1(A)) as a result of the random orientation of the ensemble of biomolecules in a liquid environment [4]. The position and relative intensity of these rings reflect the conformation of the macromolecules in solution and can be used to obtain low-resolution structural information. Given their symmetry, two-dimensional scattering patterns are usually converted to one-dimensional patterns through azimuthal averaging of detector images so as to obtain the intensity scattered by the sample as a function of the magnitude of the scattering vector ($q = 4\pi \sin\theta/\lambda$, where θ is half of the scattering angle and λ is the

(*) Corresponding author. E-mail: matteo.levantino@unipa.it

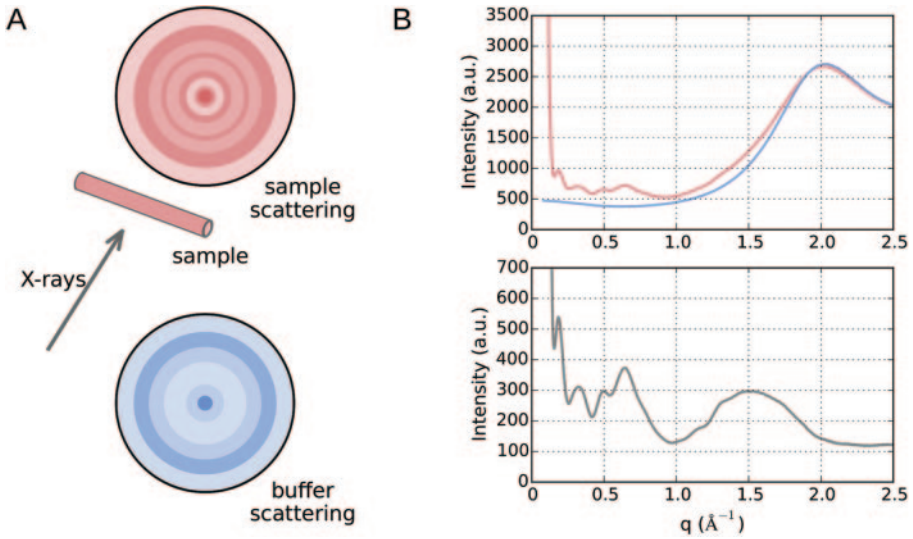

Fig. 1. – (Color online) X-ray scattering from a protein solution. (A) Schematic representation of the 2D pattern of scattered X-rays. The pattern is circularly symmetric due to the random orientation of the molecules in liquid samples. Typically both the scattering pattern of the sample (protein solution) and of the pure solvent (buffer solution) are measured. (B) Top panel: azimuthally averaged scattered intensity, $I_A(q)$, of the protein solution (red curve) and of the buffer solution, $I_B(q)$ (blue curve). Bottom panel: excess scattering intensity obtained by subtracting the buffer signal from that of the protein solution (the buffer signal was scaled to take into account the effect of solvent excluded volume according to eq. (2)). Experimental data are relative to a ∼100 mg/ml human hemoglobin solution (buffer: 0.1 M phosphate *p*H 7.4).

X-rays wavelength) (fig. 1(B)). Small-angle X-ray scattering (SAXS) for proteins typically extends up to $q \sim 0.3\,\text{Å}^{-1}$ and can be used to extract structural information with a maximum resolution of the order of 10 Å. Wide-angle X-ray solution scattering (WAXS) covers scattering angles comparable to those used in crystallographic experiments (up to $q \sim 2.5\,\text{Å}^{-1}$) and is able to provide information on protein secondary, tertiary and quaternary structures [5-8]. Even subtle changes in the packing of a protein typically result in measurable differences in the corresponding WAXS patterns [5-8]. WAXS is also sensitive to protein structural fluctuations and can be used to make an estimate of their magnitude. Indeed, an increase in protein fluctuations results in the filling of the troughs and in the reduction of the peaks of the WAXS signal [9, 10].

The availability of high-brilliant X-ray sources has recently opened the possibility to perform time-resolved WAXS (TR-WAXS) experiments [11]. In a time-resolved experiment, a protein reaction is triggered (either by a laser pulse in the case of photosensitive proteins or *e.g.* by rapid mixing of an enzyme with its substrate) and WAXS signal changes are measured at different time-delays with respect to reaction triggering. This enables to monitor in real-time even large-scale protein conformational changes that could not take place in a crystalline environment. The time-resolution of this kind of experiments can be extremely high since it is essentially determined by the duration of the triggering event and by that of the X-ray probe pulses used to monitor the structural changes taking place in the scattering volume. Modern synchrotrons and X-ray free-electron lasers (XFELs) are able to generate intense X-ray pulses with duration of ∼100 ps

and ∼10 fs, respectively, thus potentially allowing to perform TR-WAXS experiments on photoexcitable macromolecular systems with sub-ps time-resolution [12, 13]. An important milestone, relevant to both static and time-resolved X-ray solution scattering experiments, has been the development of algorithms for the calculation of solution scattering patterns using atomic coordinates determined from X-ray crystallography [14-16]. These methods have been able to yield good agreement between calculations and experimental data mainly in the SAXS region [17]. Estimating the contribution of the solvent (water in most cases) in the WAXS region is a non-trivial task, but it is essential for increasing the amount of structural and dynamic information that can be extracted from experimental signals. In the following, both advances in the computation of WAXS patterns and recent results from TR-WAXS experiments on protein solutions will be briefly reviewed.

2. – X-ray solution scattering

In standard X-ray solution scattering experiments, two sets of data are usually collected, the scattering intensity, $I_A(q)$, from the protein solution and the scattering intensity, $I_B(q)$, from pure solvent. In order to remove background scattering contributions, the pure solvent scattering intensity is typically subtracted from that of the protein solution (provided that the data are corrected for the difference in the intensity of the X-ray incident beam and for the difference in the transmission of the samples). The relevant experimental signal is thus the net excess scattering intensity

$$I(q) = I_A(q) - I_B(q). \tag{1}$$

The number of solvent molecules contained in the scattering volume during the $I_B(q)$ measurement is higher than in the case of the $I_A(q)$ measurement. This is because the solution volume is partially occupied by proteins (solvent excluded volume). While at low protein concentrations (< 10 mg/ml) the effect is small, at the typical concentrations used for WAXS measurements eq. (1) leads to a sizable oversubtraction of the solvent contribution (especially at $q > 1\,\text{Å}^{-1}$) with the excess scattering intensity becoming negative at the water scattering peak ($q \sim 2\,\text{Å}^{-1}$). For this reason, an alternative definition is the following:

$$I'(q) = I_A(q) - (1 - f)I_B(q), \tag{2}$$

where f is the excluded volume fraction [5, 18]. In the following, for simplicity, we will refer to the quantity defined by eq. (1) as the experimental signal, which is also the definition assumed by many softwares for prediction of X-ray solution scattering [16, 19]. The effect of solvent excluded volume can be anyway easily taken into account in calculations using eq. (2) and the method described below [20, 21].

The X-ray scattering intensity from a given system is essentially determined by the Fourier transform of the system electron density [22]. In particular, for system A (protein solution) and system B (pure solvent), we have that (omitting proportionality constants)

$$I_A(q) = \left\langle \left| A(\vec{q}) \right|^2 \right\rangle, \tag{3}$$

and

$$I_B(q) = \left\langle \left| B(\vec{q}) \right|^2 \right\rangle, \tag{4}$$

where $\langle \ldots \rangle$ denotes the average over all solvent and protein degrees of freedom, while the scattering amplitudes $A(\vec{q})$ and $B(\vec{q})$ are the Fourier transforms of the electron densities $\rho_A(\vec{r})$ of system A and $\rho_B(\vec{r})$ of system B, respectively,

$$A(\vec{q}) = \int \rho_A(\vec{r})\, e^{-i\vec{q}\cdot\vec{r}}\, \mathrm{d}\vec{r} \tag{5}$$

and

$$B(\vec{q}) = \int \rho_B(\vec{r})\, e^{-i\vec{q}\cdot\vec{r}}\, \mathrm{d}\vec{r}. \tag{6}$$

Structural interpretation of X-ray solution scattering data typically requires the comparison of experimental signals with those evaluated from available atomic resolution structures or from tentative structural models [23]. In many cases, the excess scattering intensity is calculated using the following expression:

$$I(q) = N \left\langle \left| A_p(\vec{q}) - \rho_0\, A_{\mathrm{excl}}(\vec{q}) + \delta\rho\, A_{\mathrm{shell}}(\vec{q}) \right|^2 \right\rangle_{\Omega}, \tag{7}$$

where $\langle \ldots \rangle_{\Omega}$ denotes the average over protein orientations, N is the number of protein molecules in the scattering volume, $A_p(\vec{q})$ is the scattering amplitude from a single protein molecule *in vacuo*, ρ_0 is the average density of the bulk solvent, $\delta\rho$ is the difference between the average density of the solvation shell surrounding the protein and that of the bulk, while $A_{\mathrm{excl}}(\vec{q})$ and $A_{\mathrm{shell}}(\vec{q})$ are the scattering amplitudes from the protein excluded volume and the solvation shell (both with unitary density), respectively [16].

Equation (7) is valid under the assumption that the protein solution is sufficiently diluted to neglect correlations between different protein molecules. It treats both the protein and solvent molecules as rigid. Moreover, it is based on the further assumption that both the bulk solvent and the solvation shells around protein molecules can be approximated as *continuous media* with uniform electron densities. While such description of the solvent is reasonable at $q \lesssim 0.1\,\text{Å}^{-1}$, where the structural resolution is low enough to neglect any solvent internal structure, the same approximation is questionable in the WAXS region. Nevertheless, predictions based on eq. (7) have proved to result in reasonably good approximations of the experimental signals of many protein solutions even at $q \sim 0.5\,\text{Å}^{-1}$ [16, 5-7, 24, 25]. Equation (7) is at the basis of the algorithms of many popular softwares such as CRYSOL [16], ORNL_SAS [26], SoftWAXS [24], FoXS [27], AXES [25] and SASTBX [28]. These softwares mainly differ in how they carry out the orientational average and evaluate the excluded volume contribution in eq. (7), which are critical aspects that determine the accuracy of the calculation, the computational time and its dependence on system size.

New approaches have been recently developed which employ atomistic descriptions of water to calculate the excess scattering intensity without resorting to the use of eq. (7) [17, 20, 21, 29]. In the following section, we will briefly summarize the main results of the derivation reported by Park *et al.* [17] in order to show how employing an atomistic description of water allows to obtain more accurate predictions in the WAXS region.

3. – X-ray scattering predictions in explicit water

As a preliminary step, note that, by separating the average over protein orientational degrees of freedom from that over all other protein and solvent degrees of freedom, the excess scattering intensity defined by eq. (1) can be written as

$$I(q) = \left\langle \left|A(\vec{q})\right|^2 \right\rangle - \left\langle \left|B(\vec{q})\right|^2 \right\rangle = \left\langle \left\langle |A(\vec{q})|^2 \right\rangle_\omega - \left\langle |B(\vec{q})|^2 \right\rangle_\omega \right\rangle_\Omega, \tag{8}$$

where, as before, $\langle \ldots \rangle_\Omega$ denotes the spherical average over different protein orientations, while $\langle \ldots \rangle_\omega$ the average over all the other protein and solvent degrees of freedom [21]. As nicely demonstrated by Park *et al.* [17], under essentially the only hypothesis that the protein solution is sufficiently diluted to neglect correlations between different protein molecules, eq. (8) is equivalent to

$$I(q) = N \left\langle D_{11}(\vec{q}) \right\rangle_\Omega, \tag{9}$$

$$\begin{aligned} D_{11}(\vec{q}) = & \left| \left\langle A_1(\vec{q}) \right\rangle_\omega - \left\langle B_1(\vec{q}) \right\rangle_\omega \right|^2 + \left[\left\langle |A_1(\vec{q})|^2 \right\rangle_\omega - \left| \left\langle A_1(\vec{q}) \right\rangle_\omega \right|^2 \right] \\ & - \left[\left\langle |B_1(\vec{q})|^2 \right\rangle_\omega - \left| \left\langle B_1(\vec{q}) \right\rangle_\omega \right|^2 \right], \end{aligned} \tag{10}$$

where $A_1(\vec{q})$ is the scattering amplitude of a single protein plus its water shell, while $B_1(\vec{q})$ is the scattering amplitude of a water droplet with the same volume and shape as that defined by the protein plus its water shell (see fig. 2).

It can be easily shown that in the *continuum*-water model eqs. (9) and (10) reduce to eq. (7). Indeed, in the framework of the *continuum*-water model, since both bulk water and water solvation shells are treated as uniform *media*, the electron density $\rho_{A1}(\vec{r})$ of

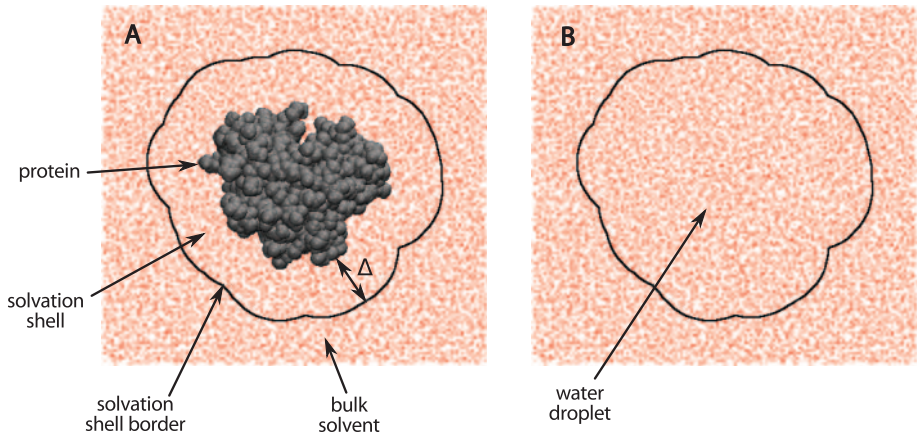

Fig. 2. – (Color online) (A) Single protein (dark gray) surrounded by water molecules (red). The continuous black line represents the envelope of the volume occupied by the protein plus its water shell. A water molecule belongs to the water shell of a protein if and only if it is within a distance Δ from any of the atoms of the protein. (B) Pure solvent. The same envelope (continuous black line) as in panel (A) defines a water droplet.

the system composed by a single protein plus its solvation shell can be written as

$$\rho_{A1}(\vec{r}) = \rho_p(\vec{r}) + \rho_{\text{shell}}\, w_{\text{shell}}(\vec{r}), \tag{11}$$

where $\rho_p(\vec{r})$ is the protein electron density, ρ_{shell} is the average density of the protein solvation shell, while $w_{\text{shell}}(\vec{r}) = 1$ if $\vec{r}$ is in the solvation shell and $= 0$ elsewhere. The electron density $\rho_{B1}(\vec{r})$ of the corresponding water droplet (fig. 2) can be written as

$$\rho_{B1}(\vec{r}) = \rho_0 \left[w_{\text{protein}}(\vec{r}) + w_{\text{shell}}(\vec{r}) \right], \tag{12}$$

where $w_{\text{protein}}(\vec{r}) = 1$ if $\vec{r}$ is in the protein and $= 0$ elsewhere. As the solvent electron density is uniform and does not fluctuate in time, the protein is implicitly approximated as a rigid body. Thus all averages in eq. (10) are immaterial. Under these hypotheses, the second and third terms in eq. (10) are vanishing and by combining eqs. (11) and (12) with eqs. (9) and (10) the excess scattering intensity reduces to

$$I(q) = N \left\langle \left| A_p(\vec{q}) - \rho_0\, A_{\text{excl}}(\vec{q}) + (\rho_{\text{shell}} - \rho_0) A_{\text{shell}}(\vec{q}) \right|^2 \right\rangle_{\Omega}, \tag{13}$$

where $A_p(\vec{q})$, $A_{\text{excl}}(\vec{q})$ and $A_{\text{shell}}(\vec{q})$ are the Fourier transforms (calculated over the protein volume) of $\rho_p(\vec{r})$, $w_p(\vec{r})$ and $w_{\text{shell}}(\vec{r})$, respectively.

Park *et al.* [17] and, more recently, Hub and coworkers [21, 30] have exploited all-atom molecular dynamics (MD) simulations to calculate the excess scattering intensity directly using eqs. (9) and (10). In particular, snapshots from MD simulations of the protein plus its hydration shell and of an equivalent droplet of pure solvent are used to directly compute the scattering amplitudes $A_1(\vec{q})$ and $B_1(\vec{q})$ before averaging the results over different simulations and molecular orientations. This approach and other physically equivalent approaches like that developed by Köfinger and Hummer [20] enable to obtain more accurate estimations of the solvent contribution to protein solution scattering [17, 21]. Moreover, since MD simulations are able to account for biomolecular motions, relevant information on protein dynamics can also be obtained [21].

Figure 3 reports a comparison between the experimental WAXS pattern of human deoxygenated hemoglobin (deoxyHb) and calculations based either on eq. (7) using the software CRYSOL (fig. 3(A)) [16] or eqs. (9) and (10) using the software WAXSiS (fig. 3(B)) [21, 30]. As can be seen from the figure, the calculation made with WAXSiS reproduces the experimental signal better than that made with CRYSOL in spite of the fact that CRYSOL (as well as other softwares based on implicit-solvent models) uses additional fitting parameters (associated with the solvation layer and the excluded solvent) to improve the match between predicted and calculated curves. By default, WAXSiS performs explicit-solvent MD simulations of the protein solution with restrained protein backbone atoms [21,30] in order to sample protein conformations close to the initial crystallographic model. Thus, while fluctuations in the protein side-chains and solvent atoms are taken into account, differences between the crystallographic protein structure and the average structure of the protein in solution may still lead to discrepancies between the data and the calculation. It is also worth noting that at $q \gtrsim 1\,\text{Å}^{-1}$, the results are sensitive to the specific explicit-water model used in the MD simulation [21]. Nevertheless, fig. 3 illustrates that, employing an atomistic description of the solvent and taking into account atomic fluctuations, good predictions of WAXS signals can be obtained without the need of introducing *ad hoc* fitting parameters, thus reducing the risk of overfittings.

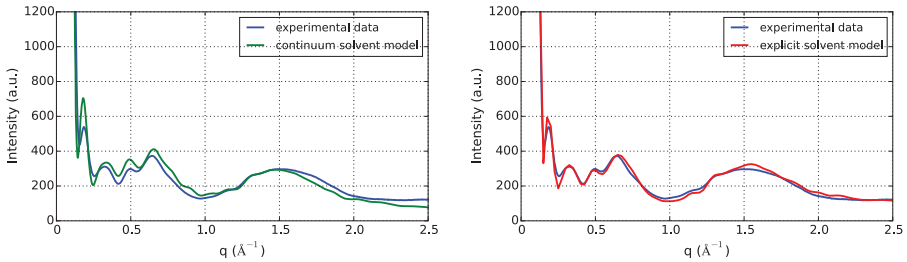

Fig. 3. – (Color online) Comparison between experimental and predicted WAXS patterns. (A) Experimental WAXS pattern of human deoxygenated hemoglobin (blue curve) and WAXS pattern calculated using CRYSOL [16] (green curve), which is based on eq. (7). (B) The same experimental pattern of panel A is compared with the prediction obtained with WAXSiS [21] (red curve), which is based on eqs. (9) and (10). In spite of the fact that no *ad hoc* fitting parameters for the solvation layer and the excluded solvent are introduced in the calculation performed with WAXSiS, the agreement with the experimental signal is better than that obtained with CRYSOL up to $q = 2.5\,\text{Å}^{-1}$.

4. – Time-resolved X-ray solution scattering

Time-resolved X-ray scattering, especially in the WAXS region, can be used to monitor as a function of time protein conformational changes occurring in solution [11]. The technique has been applied to study allosteric transitions and tertiary structural changes in both heme proteins [11, 31-35] and membrane proteins [36-39]. Here we will briefly mention the results of experiments on hemoglobin (Hb) and myoglobin (Mb), which are two emblematic examples that demonstrate the potentiality of the technique to detect even subtle protein structural changes. Hb and Mb are two heme proteins that have long served as model systems for protein dynamics studies [40-45]. Hb is able to adopt two different states characterized by different quaternary structures, the R or "relaxed" state and the T or "tense" state [46-51]. In solution, breakage of the bonds between Hb and its ligands triggers the transition from the R to the T state. The main structural change associated to the R-T transition, *i.e.* the relative rotation of the two Hb dimers, is clearly detected with TR-WAXS (fig. 4(A)) [11, 52]. Moreover, the experimental data can be accurately described in terms of a linear combination of the deoxyHb (T-state) and HbCO (R-state) WAXS signals [11, 52]. When, as in the Hb case, a clear structural attribution of the observed signals is obtained, the time evolution of the data can be tested against different alternative kinetic models and accurate estimation of the rate of conformational changes are obtained [32]. Remarkably, in the case of Hb, it was possible to show that the rate of the R-T transition is $\sim$1 μs, *i.e.* more than an order of magnitude faster than previously assumed on the basis of time-resolved optical spectroscopic data [52-56], as recently confirmed also by the transient grating technique [57].

Mb is a monomeric protein that undergoes a series of tertiary relaxation after ligand photolysis [59-62]. The high sensitivity of time-resolved X-ray scattering has been recently demonstrated with an experiment on Mb (fig. 4(B)) performed at the Linear Coherent Light Source (SLAC National Accelerator Laboratory) [35]. In this case, thanks to the unprecedented time-resolution achievable at XFELs, it was possible to show that Mb undergoes an ultrafast proteinquake [64] in $\sim$1 ps followed by damped oscillations of the entire protein globular structure in the ps time-scale [35]. The observation of coherent oscillatory behavior at a specific vibrational frequency is remarkable from a physical

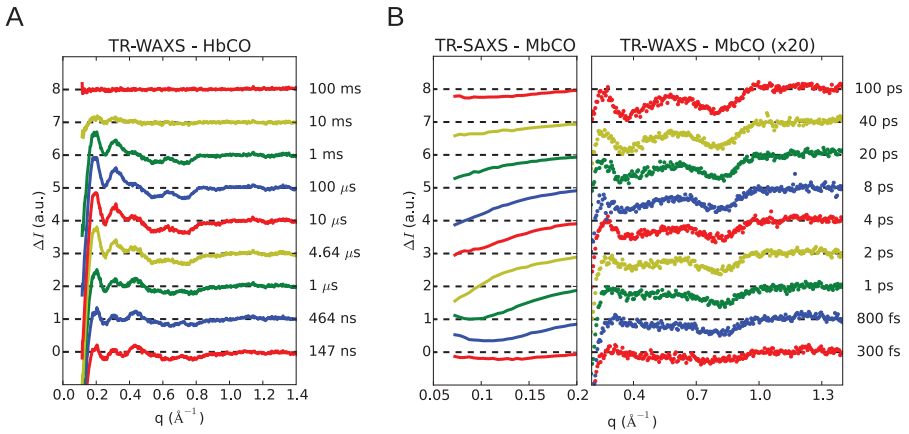

Fig. 4. – (Color online) Time-resolved X-ray difference scattering curves of (A) carbonmonoxy hemoglobin and (B) carbonmonoxy myoglobin, after photolysis of the bond(s) between the protein and the ligand(s). At each time-delay the signal is the difference between the scattering pattern of the sample and that at a reference time-delay before photoexcitation. In the case of the Hb experiment, a ∼200 ns photolysis pulse was used and data were acquired at the ID09 beamline of the European Synchrotron Radiation Facility (ESRF) in Grenoble [52]. Mb data were acquired at the XPP beamline of the Linear Coherent Light Source (LCLS, SLAC National Accelerator Laboratory) and a ∼250 fs photolysis pulse was used [35]. The LCLS X-ray free-electron laser is capable of producing extremely short (∼30 fs) and intense X-ray pulses [58].

point of view. Indeed, it is generally assumed that low frequency collective vibrations, like the one observed in the XFEL experiment, would be overdamped in water. The data reported in ref. [35] clearly ruled out this assumption. There are several possible physical mechanisms that could explain this experimental observation (*e.g.* activation of a specific single protein vibrational mode or anharmonic combination of several protein vibrational modes) and further investigations are needed to discern between different models.

It is worth stressing that there is a fundamental difference in the kind of physical process underlying the time evolutions observed in the cases of Hb (fig. 4(A)) and in that of Mb (fig. 4(B)). The signal changes in the Hb experiment are due to a kinetic process: the system explores initially (at ∼100 ns from photolysis) an intermediate state (R-state deoxyHb) before populating the equilibrium state (T-state deoxyHb) in the microsecond time-scale. In the case of the Mb experiment, which probed a much shorter time-scale, the time evolution of the data is due to a dynamical process: the ensemble of proteins in the scattering volume undergoes a coherent oscillatory motion in the picosecond time-scale after the (synchronizing) photolysis pulse. The tracked ultrafast motion of Mb molecules is not an activated process in the sense that Mb molecules do not have to overcome energy barriers to explore different states (free-energy minima). The observation of such dynamical process was possible thanks to the structural sensitivity of TR-SAXS/WAXS and to the unprecedented time-resolution achievable at the LCLS [65].

5. – Conclusions

X-ray solution scattering has enough structural sensitivity to probe macromolecular motions ranging from large-scale conformational changes to more localized tertiary

relaxations. Time-resolved measurements allow to probe such structural rearrangements in real time, thus yielding accurate measurements of the rates of conformational changes. In order to increase the amount of structural and dynamic information that can be extracted from experimental signals, methods that better take into account the solvent contribution and biomolecular dynamics are currently being developed. The advent of XFELs offers nowadays the possibility of exploring the ultrafast structural dynamics of proteins with sub-ps time resolution.

* * *

This paper is dedicated to Prof. Sow-Hsin Chen in the occasion of his 80th birthday, to celebrate his outstanding career and scientific achievements. We acknwoledge Dr. Marco Cammarata for stimulating discussions, helpful suggestions, and for his decisive contribution to the development of the TR-WAXS technique. M. L. would like to acknowledge the support from COST Action CM1306 "Understanding Movement and Mechanism in Molecular Machines".

REFERENCES

[1] Karplus M. and Kuriyan J., *Proc. Natl. Acad. Sci. U.S.A.*, **102** (2005) 6679, http://dx.doi.org/10.1073/pnas.0408930102.
[2] Henzler-Wildman K. and Kern D., *Nature*, **450** (2007) 964, http://dx.doi.org/10.1038/nature06522.
[3] Kamerlin S. C. and Warshel A., *Proteins*, **78** (2010) 1339, http://dx.doi.org/10.1002/prot.22654.
[4] Als-Nielsen J. and McMorrow D., *Elements of Modern X-ray Physics*, 2nd edition (John Wiley ans Sons) 2011.
[5] Hirai H. *et al.*, *J. Synchrotron Radiat.*, **9** (2002) 202, http://dx.doi.org/10.1107/S0909049502006593.
[6] Fischetti R. D. *et al.*, *Chem. Biol.*, **11** (2004) 1431, http://dx.doi.org/10.1016/j.chembiol.2004.08.013.
[7] Makowski L. *et al.*, *J. Mol. Biol.*, **383** (2008) 731, http://dx.doi.org/10.1016/j.jmb.2008.08.038.
[8] Elshemey W. M. *et al.*, *Protein J.*, **29** (2010) 545, http://dx.doi.org/10.1007/s10930-010-9291-z.
[9] Makowski L. *et al.*, *J. Mol. Biol.*, **375** (2008) 529, http://dx.doi.org/10.1016/j.jmb.2007.07.075.
[10] Makowski L. *et al.*, *Biopolymers*, **95** (2011) 531, http://dx.doi.org/10.1002/bip.21631.
[11] Cammarata M. *et al.*, *Nat. Methods*, **5** (2008) 881, http://dx.doi.org/10.1038/nmeth.1255.
[12] Neutze R. and Moffat K., *Curr. Opin. Struct. Biol.*, **22** (2012) 651, http://dx.doi.org/10.1002/bip.360220607.
[13] Levantino M. *et al.*, *Curr. Opin. Struct. Biol.*, **35** (2015) 41, http://dx.doi.org/10.1016/j.sbi.2015.07.017.
[14] Fedorov B. A. *et al.*, *FEBS Lett.*, **28** (1972) 188, http://dx.doi.org/10.1016/0014-5793(72)80708-7.
[15] Pavlov M. Y. and Fedorov B. A., *Biopolymers*, **22** (1983) 1507, http://dx.doi.org/10.1002/bip.360220607.
[16] Svergun D. I. *et al.*, *J. Appl. Crystallogr.*, **28** (1995) 768, http://dx.doi.org/10.1107/S1600536804004209.
[17] Park S. *et al.*, *J. Chem. Phys.*, **130** (2009) 134114, http://dx.doi.org/10.1063/1.3099611.

[18] Makowski L., *J. Struct. Funct. Genomics*, **11** (2010) 9, http://dx.doi.org/10.1007/s10969-009-9075-x.
[19] Schneidman-Duhovny D. *et al.*, *Biophys J.*, **105** (2013) 962, http://dx.doi.org/10.1016/j.bpj.2013.07.020.
[20] Kofinger J. and Hummer G., *Phys. Rev. E*, **87** (2013) 052712, http://dx.doi.org/10.1103/PhysRevE.87.052712.
[21] Chen P.-C. and Hub J. S., *Biophys. J.*, **107** (2014) 435, http://dx.doi.org/10.1016/j.bpj.2014.06.006.
[22] Chen S.-H. and Tartaglia P., *Scattering Methods in Complex Fluids*, 1st edition (Cambridge University Press) 2015.
[23] Spilotros A. and Svergun D. I., in *Encyclopedia of Analytical Chemistry* (John Wiley and Sons) 2014, pp. 1–34, http://dx.doi.org/10.1002/9780470027318.a9447.
[24] Bardhan J. P. *et al.*, *J. Appl. Crystallogr.*, **42** (2009) 932, http://dx.doi.org/10.1107/S0021889809032919.
[25] Grishaev A. *et al.*, *J. Am. Chem. Soc.*, **132** (2010) 15484, http://dx.doi.org/10.1021/ja106173n.
[26] Tjioe E. and Heller W. T., *J. Appl. Crystallogr.*, **40** (2007) 782, http://dx.doi.org/10.1107/S002188980702420X.
[27] Schneidman-Duhovny D. *et al.*, *Nucl. Acids Res.*, **38** (2010) W540, http://dx.doi.org/10.1093/nar/gkq461.
[28] Liu H. *et al.*, *J. Appl. Crystallogr.*, **45** (2012) 587, http://dx.doi.org/10.1107/S0021889812015786.
[29] Tong D. *et al.*, *J. Appl. Crystallogr.*, **48** (2014) 1834, http://dx.doi.org/10.1107/S1600576715018816.
[30] Knight C. J. and Hub J. S., *Nucl. Acids Res.*, **43** (2015) W225, http://dx.doi.org/10.1093/nar/gkv309.
[31] Cho H. S. *et al.*, *Proc. Natl. Acad. Sci. U.S.A.*, **107** (2010) 7281, http://dx.doi.org/10.1073/pnas.1002951107.
[32] Levantino M. *et al.*, *Proc. Natl. Acad. Sci. U.S.A.*, **109** (2012) 14894, http://dx.doi.org/10.1073/pnas.1205809109.
[33] Kim T. W. *et al.*, *J. Am. Chem. Soc.*, **134** (2012) 3145, http://dx.doi.org/10.1021/ja210435n.
[34] Spilotros A. *et al.*, *Soft Matter*, **8** (2012) 6434, http://dx.doi.org/10.1039/C2SM25676B.
[35] Levantino M. *et al.*, *Nat. Commun.*, **6** (2015) 6772, http://dx.doi.org/10.1038/ncomms7772.
[36] Andersson M. *et al.*, *Structure*, **17** (2009) 1265, http://dx.doi.org/10.1016/j.str.2009.07.007.
[37] Malmerberg E. *et al.*, *Biophys. J.*, **101** (2011) 1345, http://dx.doi.org/10.1016/j.bpj.2011.07.050.
[38] Takala H. *et al.*, *Nature*, **509** (2014) 245, http://dx.doi.org/10.1038/nature13310.
[39] Malmerberg E. *et al.*, *Sci. Signal*, **8** (2015) ra26, http://dx.doi.org/10.1126/scisignal.2005646.
[40] Bellelli A. and Brunori M., *Biochim. Biophys. Acta*, **1807** (2011) 1262, http://dx.doi.org/10.1016/j.bbabio.2011.04.004.
[41] Yonetani T. and Laberge M., *Biochim. Biophys. Acta*, **1784** (2008) 1146, http://dx.doi.org/10.1016/j.bbapap.2008.04.025.
[42] Changeux J.-P., *Annu. Rev. Biophys.*, **41** (2012) 103, http://dx.doi.org/10.1146/annurev-biophys-050511-102222.
[43] Yuan Y. *et al.*, *Chem. Rev.*, **115** (2015) 1702, http://dx.doi.org/10.1021/cr500495x.
[44] Frauenfelder H. *et al.*, *Proc. Natl. Acad. Sci. U.S.A.*, **100** (2003) 8615, http://dx.doi.org/10.1073/pnas.1633688100.
[45] Brunori M. *et al.*, *Methods Enzymol.*, **437** (2008) 1047, http://dx.doi.org/10.1016/S0076-6879(07)37020-1.

[46] Brzozowski A. *et al.*, *Nature*, **307** (1984) 74, http://dx.doi.org/10.1038/307074a0.
[47] Shibayama N. and Saigo S., *J. Mol. Biol.*, **251** (1995) 203, http://dx.doi.org/10.1006/jmbi.1995.0427.
[48] Levantino M. *et al.*, *Biochemistry*, **42** (2003) 4499, http://dx.doi.org/10.1021/bi0272555.
[49] Viappiani C. *et al.*, *Proc. Natl. Acad. Sci. U.S.A.*, **101** (2004) 14414, http://dx.doi.org/10.1073/pnas.0405987101.
[50] Park S. Y. *et al.*, *J. Mol. Biol.*, **360** (2006) 690, http://dx.doi.org/10.1016/j.jmb.2006.05.036.
[51] Ronda L. *et al.*, *Curr. Org. Chem.*, **19** (2015) 1653, http://dx.doi.org/10.2174/1385272819666150601211349.
[52] Cammarata M. *et al.*, *J. Mol. Biol.*, **400** (2010) 951, http://dx.doi.org/10.1016/j.jmb.2010.05.057.
[53] Spiro T. G. and Balakrishnan G., *J. Mol. Biol.*, **400** (2010) 949, http://dx.doi.org/10.1016/j.jmb.2010.05.056.
[54] Hofrichter J. *et al.*, *Proc. Natl. Acad. Sci. U.S.A.*, **80** (1983) 2235, http://dx.doi.org/10.1073/pnas.80.8.2235.
[55] Goldbeck R. A. *et al.*, *Biochemistry*, **35** (1996) 8628, http://dx.doi.org/10.1021/bi952248k.
[56] Balakrishnan G. *et al.*, *J. Mol. Biol.*, **340** (2004) 843, http://dx.doi.org/10.1016/j.jmb.2004.05.012.
[57] Yang C. *et al.*, *Phys. Chem. Chem. Phys.*, **17** (2015) 22571, http://dx.doi.org/10.1039/C5CP03059E.
[58] Levantino M. *et al.*, *Struct. Dyn.*, **2** (2015) 041713, http://dx.doi.org/10.1063/1.4921907.
[59] Schotte F. *et al.*, *Science*, **300** (2013) 1944, http://dx.doi.org/10.1126/science.1078797.
[60] Bourgeois D. *et al.*, *Proc. Natl. Acad. Sci. U.S.A.*, **100** (2003) 8704, http://dx.doi.org/10.1073/pnas.1430900100.
[61] Levantino M. *et al.*, *Proc. Natl. Acad. Sci. U.S.A.*, **101** (2004) 14402, http://dx.doi.org/10.1073/pnas.0406062101.
[62] Dantsker D. *et al.*, *Biochim. Biophys. Acta*, **1749** (2005) 234, http://dx.doi.org/10.1016/j.bbapap.2005.04.002.
[63] Kim K. H. *et al.*, *Chem. Commun.*, **47** (2011) 289, http://dx.doi.org/10.1039/c0cc01817a.
[64] Ansari A. *et al.*, *Proc. Natl. Acad. Sci. U.S.A.*, **85** (1985) 5000, http://dx.doi.org/10.1073/pnas.82.15.5000.
[65] Bostedt C. *et al.*, *Rev. Mod. Phys.*, **88** (2016) 152021, http://dx.doi.org/10.1103/RevModPhys.88.015007.